Enhanced Interfacial Properties of High-Modulus Carbon Fiber Reinforced PEKK Composites by a Two-Step Surface Treatment: Electrochemical Oxidation Followed by Thermoplastic Sizing

Meng Zhang[1,2] · Xin Qian[1] · Kai Ma[1] · Hongbo Ma[1] · Yonggang Zhang[1]

Abstract

A two-step surface treatment was conducted on high strength and high modulus carbon fibers (HSHM-CFs) to enhance the interfacial properties of polyetherketoneketone (PEKK) matrix composites. In the two-step surface treatment, the surfaces of HSHM-CFs were electrochemically oxidized followed by sizing treatment. Thermoset epoxy (EP) sizing agents and thermoplastic polyetherimide (PEI) sizing agents were utilized for comparison. Results showed that PEI sizing agents had better wetting effects than EP sizing agents. The sizing process led to increases in fiber strength due to healed surface flaws and inhibited micro-crack initiation. Although EP sizing agents were incompatible with PEKK matrix, the interlaminar shear strength (ILSS) of PEKK matrix composites reinforced by EP-sized fibers still increased, compared with that by untreated fibers, due to hydrogen bond and weak chemical reactions between HSHM-CFs and PEKK matrix. The strong interaction between PEI sizing agents and HSHM-CFs, diffusion and entanglement as well as the non-covalent π-π interaction between PEI sizing agents and PEKK matrix resulted in highest ILSS value of PEI-sized HSHM-CF/PEKK composites.

Meng Zhang and Xin Qian contributed equally to this work and should be considered co-first authors.

✉ Xin Qian
   qx3023@nimte.ac.cn

✉ Yonggang Zhang
   zhangyonggang@nimte.ac.cn

1   National Engineering Laboratory of Carbon Fiber Preparation Technology, Ningbo Institute of Materials Technology and Engineering, Chinese Academy of Sciences, Ningbo 315201, Zhejiang, China

2   School of Materials Science and Engineering, Henan Polytechnic University, Jiaozuo 454000, China

1 Introduction

Owing to high-temperature stability and superior impact strength, high-performance polyaryletherketones (PAEK) polymers have attracted significant interest [1, 2]. In general, the PAEK polymers consist of several plastics, such as polyetheretherketone (PEEK), polyetherketoneketone (PEKK), polyetherketone (PEK), polyetheretherketoneketone (PEEKK), and so on [3–6]. As a family of semi-crystalline thermo-plastics, PEEK and PEKK polymers have many outstanding properties such as better resistance to creep deformation, excellent thermal stability, good resistance to chemicals and solvents, and flame retardancy [7–12]. During the past decades, carbon fiber (CF) reinforced PEEK composites have been widely used in aviation and aerospace [13–15]. Compared with PEEK polymer, PEKK is relatively new to the market. However, PEKK attains more and more attention due to its superior thermal and mechanical properties [3, 6, 16], e.g. PEKK has a relatively higher glass transition temperature T_g (>165 °C) and melting temperature T_m (>360 °C) than those of PEEK ($T_g \approx 143$ °C and $T_m \approx 343$ °C) [17], and PEKK composites also have lower processing temperatures than PEEK composites [18].

However, the applications of CF/PEKK composites are somewhat limited due to the chemical inertness of CFs and poor wettability between CFs and PEKK matrix. So far, there is a lack of investigations on the interfacial properties between CFs and PEKK [3], and many researches focus on the preparation and properties of CF/PEEK composites [10–17, 19–28]. In order to improve the interfacial properties of CF/PEEK composites, various types of surface treatment methods have been conducted onto CF surfaces such as liquid-phase oxidation [19], plasma treatment [20, 21], gas oxidation [22, 23] and grafting functional groups [15, 24]. In addition, the sizing treatment also has been utilized to enhance the interfacial adhesion of CF/PEEK composites [12, 13, 25–28]. However, commercially available sizing agents are mainly epoxy-type (EP) sizing agents. The degradation temperature (about 250 °C) of EP sizing agents is significantly lower than the processing temperature of PEEK and PEKK, which are possibly incompatible with PEEK and PEKK matrix [29]. As a result, the sizing agents with a similar chemical structure to PEEK and PEKK are generated to endow good interfacial compatibility between CFs and PEEK and PEKK matrix.

As one kind of thermoplastic polymer, polyetherimide (PEI) has the miscible feature to PEEK and PEKK, and its chains can also spread to PEEK and PEKK chains at high processing temperature and pressure [30–32]. Meanwhile, PEI sizing agents have also been confirmed to effectively enhance the interfacial adhesion of CF/PEEK composites. According to the research by Giraud et al. [33, 34], an aqueous dispersion of PEI resulted in very stable sizing agent and it also had better interface adhesion. Research by Hassan et al. indicated that the coating with a mixture of PEI and functionalized multi-walled carbon nanotubes onto CF surfaces led to remarkable improvement in the ILSS of modified CF/PEEK composites, which resulted from the combination of hydrogen bonding between carbon nanotubes and PEI as well as the π-π interaction between PEI and PEEK [25]. The interfacial bonding of CF/PEEK composites could also be improved by applying PEI and graphene oxide complex sizing at the interface [13].

Previous published works on CF/PEKK composites also mainly focus on reinforcing CFs with standard tensile modulus around 230 GPa, such as Hexcel AS4 CFs [35–38]. In the present work, high strength and high modulus CFs (HSHM-CFs) with the tensile strength and the tensile modulus around 5.0 GPa and 310 GPa, respectively,

were prepared through a continuous production line and taken as the reinforcing fibers of PEKK matrix composites. Much higher tensile modulus of HSHM-CFs than that of standard modulus CFs resulted in much more inert surfaces. In our previous studies [39–44], surface electrochemical oxidation of CFs was confirmed to significantly improve the interfacial bonding strength of CF reinforced matrix composites. Therefore, in order to obtain improved interfacial properties of HSHM-CF/PEKK composites, the electrochemical oxidation followed by thermoplastic sizing treatment was employed to modify the fiber surfaces.

The aim of this study was to evaluate the synergy of electrochemical surface oxidation and thermoplastic PEI sizing agents on the interfacial properties of HSHM-CF/PEKK composites. Commercial EP sizing agents were also coated onto HSHM-CF surfaces after electrochemical oxidation for comparison. The electrochemical oxidation and sizing were processed by a series of continuous devices. Scanning electron microscopy (SEM) and X-ray photoelectron spectroscopy (XPS) were employed to monitor surface physical–chemical properties of HSHM-CF before and after surface modification. Interfacial enhancement mechanism of PEKK matrix composites reinforced by electrochemically oxidized fibers, EP-sized fibers and PEI sized fibers were discussed in detail.

2 Experiment

2.1 Materials

PAN-based HSHM-CFs were produced in our laboratory according to a continuous process, which was composed of preparation of PAN-precursors, stabilization (180 °C-270 °C, air atmosphere), low temperature carbonization (300 °C-800 °C, nitrogen atmosphere), high temperature carbonization (1000 °C-1500°C, nitrogen atmosphere) and graphitization (2000 °C, argon atmosphere). There were 6000 filaments in per tow and the typical diameter of each filament was approximately 5.0 μm. During the electrochemical process of HSHM-CFs, ammonium bicarbonate (NH_4HCO_3, analytical purity) was taken as the electrolyte, which was purchased from Sinopharm Chemical Reagent Co. (Shanghai, China) [45]. PEKK powders were obtained from Shandong Kaisheng New Materials Co. Ltd., and m-Phenylenediamine (MPD, analytical purity 99%) were purchased from Aladdin Co. Ltd., China. 1,2-Dichlorobenzene (analytical purity) was supplied by Sinopharm Chemical Reagent Co., and 4,4'-(4,4'-isopropylidenediphenoxy)bis-(phthalic anhydride) (BPADA) was purchased from Changzhou Sunlight Pharmaceutical Co., Ltd., China.

2.2 The Surface Treatment of HSHM-CFs

Electrochemical surface oxidation of HSHM-CFs was conducted in a custom-built laboratory set-up with an aqueous 5.0 wt% NH_4HCO_3 solution as the electrolyte. The residence time of HSHM-CFs in the surface treatment bath was 90 s (running speed 1.0 m/min) with the electric current density of 1.0 A/m². After the oxidation, HSHM-CFs were washed with deionized water in the washing bath followed by further drying in an oven at 110 °C for 90 s.

PEI resin was prepared by the polymerization reaction of MPD as diamine and equimolar amounts of BPADA as dianhydride in N-methyl-2-pyrrolidone (NMP) solution, and the synthesized process was as shown in Scheme 1. The standard protocol of solution
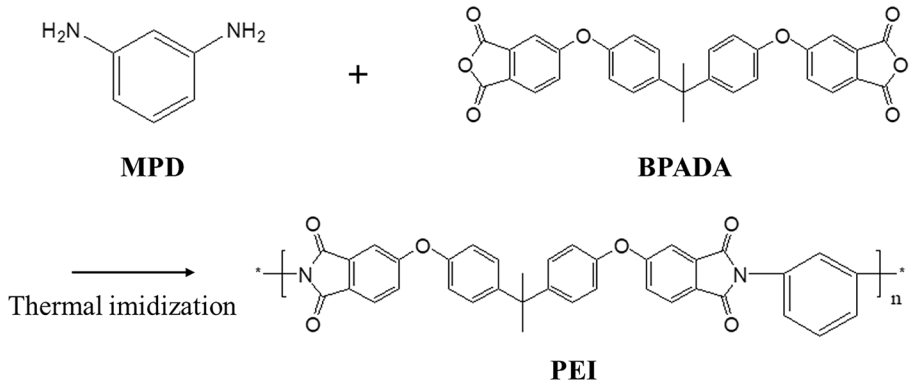
Scheme 1 Polymerization process of polyetherimide (PEI) resin

polymerization technique was adopted as reported elsewhere [46]. A magnetic stirrer and Dean-Stark trap fitted with a condenser was charged with 41.34 g (79.537 mmol) of BPADA and 8.60 g (79.537 mmol) of MPD in 180 mL 1,2-dichlorobenzene under constant flow of nitrogen. The typical reaction time was 6 h at 180 °C and then cooled to room temperature. 1.0% PEI sizing agent was obtained through a mixture of synthesized PEI and water.

A two-step surface treatment including surface electrochemical oxidation followed by sizing process was conducted onto HSHM-CF surfaces. In the sizing process, synthesized PEI sizing agents and commercial EP sizing agents (Zhongfang Haitian Co. Ltd., Beijing, China) were chosen as agents, respectively. The schematic representation of the continuous surface treatment is shown in Fig. 1. The corresponding samples untreated HSHM-CFs, electrochemically oxidized HSHM-CFs, EP sized HSHM-CFs after surface electrochemical oxidation and PEI sized HSHM-CFs after surface electrochemical oxidation were denoted as HSHM-CF, HSHM-CF@O, HSHM-CF@EP and HSHM-CF@PEI, respectively.
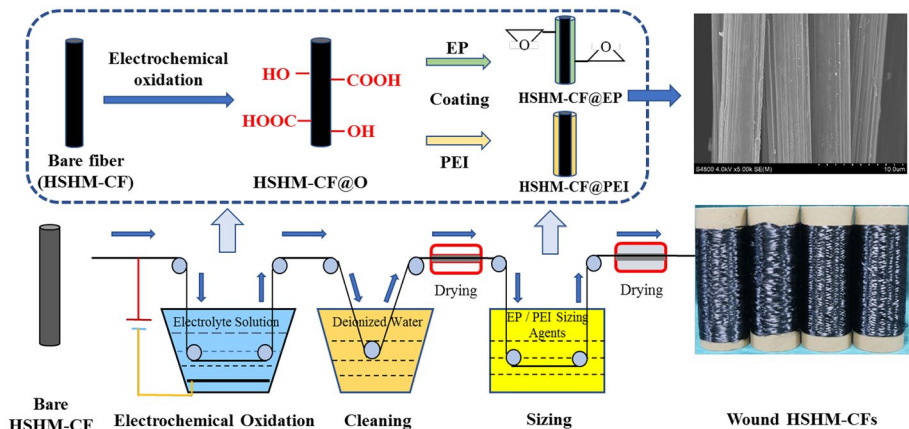

Fig. 1 Schematic diagram of continuous surface treatment

2.3 Preparation of HSHM-CF/PEKK Composites

Four kinds of HSHM-CF samples (untreated HSHM-CF, HSHM-CF@O, HSHM-CF@ EP and HSHM-CF@PEI) made in our laboratory were chosen as the reinforcing fibers of PEKK matrix composites. HSHM-CF samples were laid flat on a metal mould and unidirectional HSHM-CF/PEKK prepreg was obtained by melt impregnation of PEKK onto fiber surfaces for 20 min at 350 °C in ambient air. HSHM-CF/PEKK composite laminates were composed of 8 plies of unidirectional prepreg with the size of 80 mm × 100 mm. The laminates were processed by hot press at 340 °C with a pressure of 1.25 MPa for 20 min. Subsequently, the laminates were gradually cooled to room temperature with a cooling rate of 10 °C/ min. The total volume fraction of HSHM-CFs in PEKK matrix composites was approximately 60% and the thickness of final composite sample was 2 mm. The schematic representation of the preparation process of HSHM-CF/PEKK composites is shown in Fig. 2.

2.4 Characterization of Surface Physicochemical Structure

Surface and cross-sectional morphologies of HSHM-CFs before and after surface treatment were observed using a Hitachi S-4800 model scanning electron microscope (SEM) with acceleration voltage of 4 kV. The fiber samples were sputter-coated with gold before imaging [47]. X-ray photoelectron spectroscopy (XPS) measurements were conducted on an Axis Ultra DLD model X-ray photoelectron spectroscopy (XPS) with an achromatic Mg Kα X-ray as radiation source. The emission current was 30 mA with the voltage of 15 kV [48]. Curve fitting was carried out using a nonlinear least squares fitting program with a Gaussian/Lorentzian sum function. The C1s binding energy corresponding to graphitic carbon was referenced at 284.6 eV for calibration [49, 50].
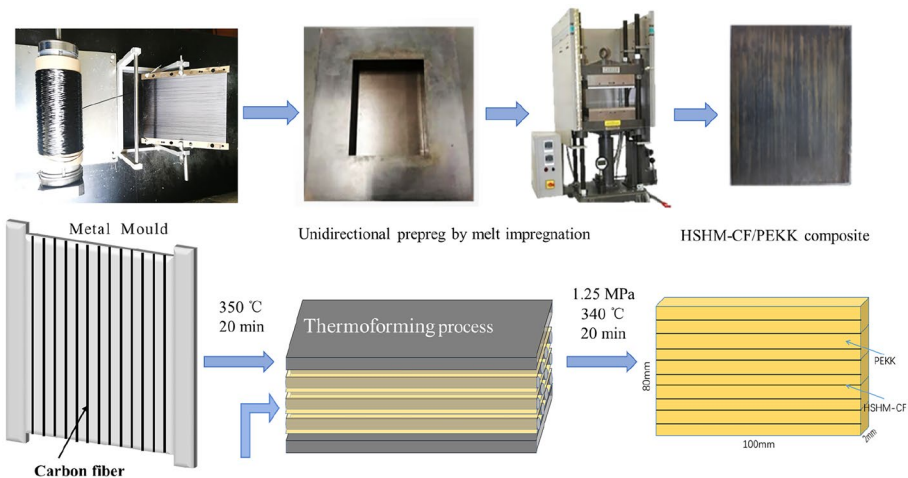

Fig. 2 Schematic diagram of preparation process of HSHM-CF/PEKK composites

2.5 Mechanical Properties of HSHM-CF and HSHM-CF/PEKK Composites

The tensile strength and tensile modulus of HSHM-CFs before and after surface treatment were evaluated according to ASTM D4018-17. A universal testing machine (model 5569A, Instron Corp.) at a crosshead speed of 10.0 mm/min with the gauge length of 150 mm was utilized, and at least eight specimens were tested for each sample.

The ILSS values of HSHM-CF/PEKK composites were determined by a three-point short beam bending test method. The tests were performed on a model 3366 universal material testing machine (Instron Corp.) according to ASTM D 2344. The crosshead speed was of 1.0 mm/min. More than eight specimens were tested for each of the samples. In addition, the fracture morphologies of HSHM-CF/PEKK composites were also observed through SEM images. The ILSS values of HSHM-CF/PEKK composites were calculated from the equation [43]:

$$ILSS = \frac{3F_{max}}{4b \times d}$$

where F_{max} is the maximum load, b the width of the test samples, and d the thickness of the test samples.

3 Results and Discussion

3.1 Surface Morphological Analysis

Figure 3 illustrates the surface and cross-sectional SEM images of untreated HSHM-CF (HSHM-CF), electrochemically oxidized HSHM-CF (HSHM-CF@O), epoxy sized HSHM-CF after surface electrochemical oxidation (HSHM-CF@EP) and PEI sized HSHM-CF after surface electrochemical oxidation (HSHM-CF@PEI). It could be observed from Fig. 3a that longitudinal ridges and striations running along the length of fibers were found on the surfaces of untreated HSHM-CF. The characteristic grooves resulted from the wet spinning process of PAN-precursors due to skin forming and diffusion of solvents out from the core [51]. In addition, the abundance of granules observed on untreated HSHM-CF surface and cross-section were possibly attributed to the pyrolytic by-products or impurities absorbed in the manufacturing process [39, 52].

Compared with untreated HSHM-CF, characteristic longitudinal ridges became much more well-defined, and the contaminants were also absent on the surfaces of electrochemically oxidized HSHM-CF@O sample (Fig. 3b). Our previous studies had proven that the electrochemical oxidation could get rid of foreign contaminants on the fiber surfaces [39, 41, 45]. Obvious sizing agents could be found from surface and cross-sectional SEM images of HSHM-CF@EP sample and HSHM-CF@PEI sample (Fig. 3c-d). As shown in SEM images at lower magnification, longitudinal ridges on the surfaces of HSHM-CF@EP sample became less well-defined due to the introduction of epoxy sizing agents (Fig. 3e). As for the HSHM-CF@PEI sample, SEM images at lower magnification reviewed that the sizing agents covered the fiber surfaces more evenly than that of HSHM-CF@EP sample (Fig. 3f), which indicated that PEI sizing agent could better form a layer on the surfaces of carbon fiber.
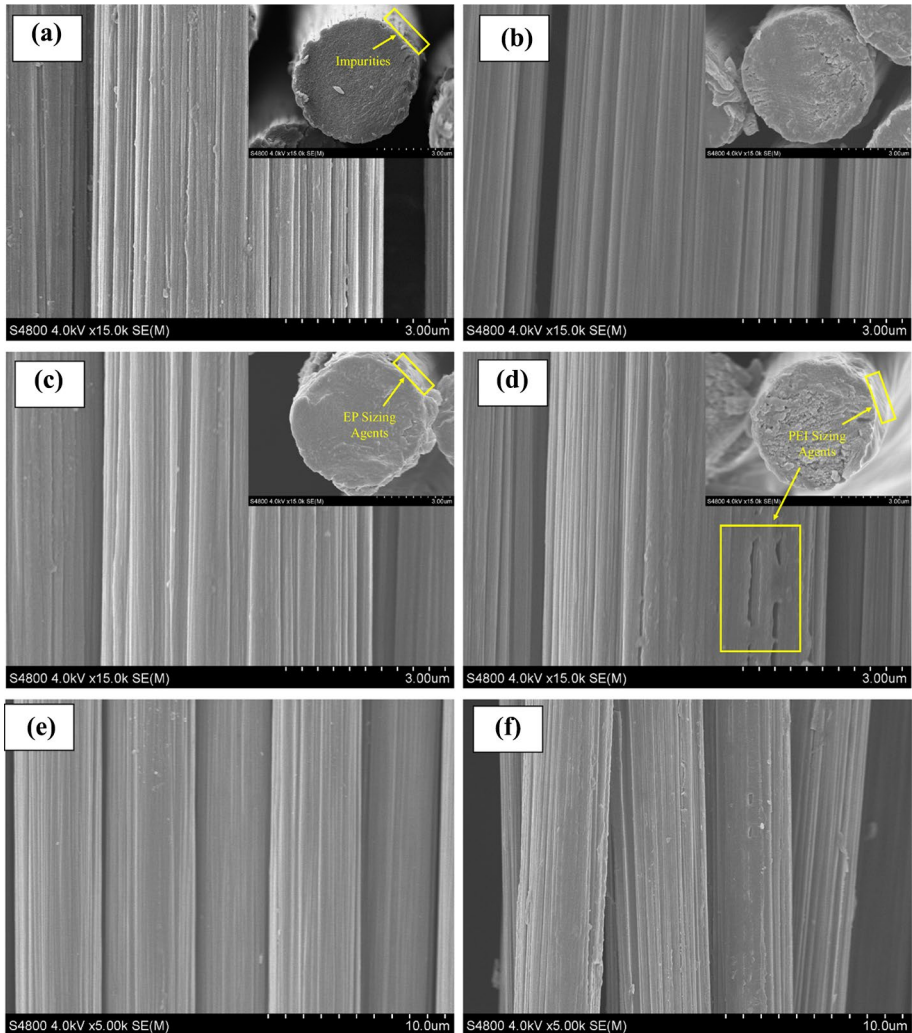
Fig. 3 The surface and the cross-sectional SEM images of (**a**) untreated HSHM-CF sample, (**b**) HSHM-CF@O sample, (**c**) HSHM-CF@EP sample, (**d**) HSHM-CF@PEI sample, (**e**) HSHM-CF@EP sample at lower magnification, and (**f**) HSHM-CF@PEI sample at lower magnification

3.2 Surface Chemical Compositions by XPS

High-resolution XPS spectra and surface element composition of HSHM-CFs before and after surface treatment are shown in Fig. 4. The characteristic peaks in the XPS spectra of HSHM-CFs at 284.6 eV, 532.6 eV and 102.6 eV indicated the C1s peak, O1s peak and Si2p peak, respectively, which confirmed that surface elements of untreated fibers were mainly composed of carbon, oxygen and silicon [53]. The relative contents of C and O on the surfaces of untreated HSHM-CF were 93.81% and 4.90%, respectively, and extremely high content of inert carbon element proved that untreated fibers had highly
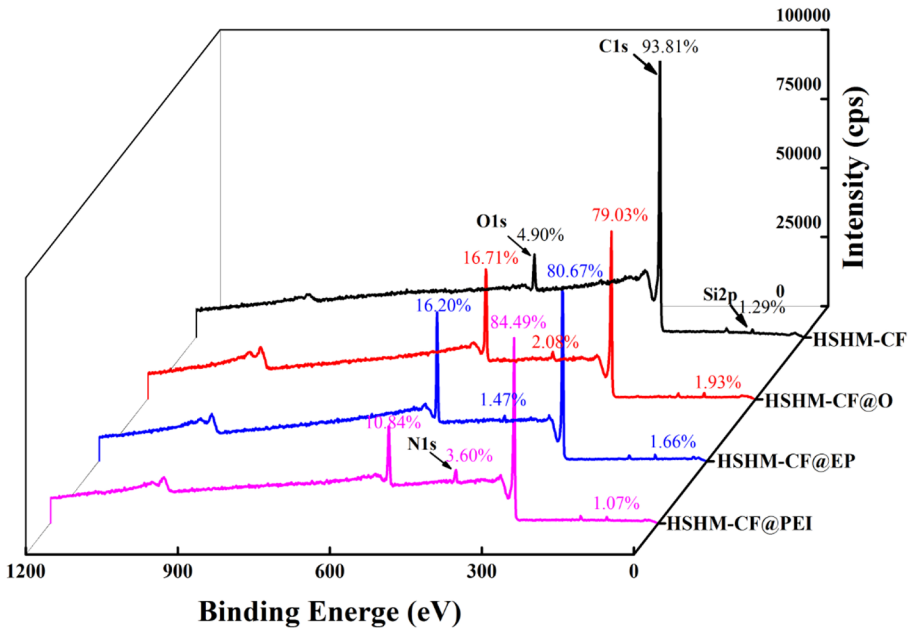
Fig. 4 High resolution XPS spectra of untreated HSHM-CF sample, HSHM-CF@O sample, HSHM-CF@EP sample and HSHM-CF@PEI sample

inert surfaces. A small quantity of silicon element could be attributed to silicone oil contamination in the production of PAN precursors [41]. After surface electrochemical oxidation, the relative content of O on the surfaces of HSHM-CF@O sample increased by 241% compared with untreated HSHM-CF. The relative content of C also decreased from 93.81% to 79.03%. In addition, the N element with the percentage of 2.08% was also introduced onto fiber surfaces. Outer weak boundary layer could be removed during the process of electrochemical oxidation [28, 39], and the internal higher content of Si could be detected. As a result, the relative content of Si increased from 1.29% to 1.93% after electrochemical oxidation. Increased relative contents of polar O and N elements indicated that the oxidized HSHM-CF surfaces became much more active due to surface electrochemical oxidation.

As also can be seen from Fig. 4, both EP-sizing and PEI-sizing process resulted in increased percentage of C element and decreased percentage of O element, especially for the surfaces of PEI-sized HSHM-CF@PEI sample, the relative content of O element decreased by 35% and the relative content of C element increased by 7% compared with that of electrochemically oxidized HSHM-CF@O sample. This resulted from the introduction of functional groups of PEI sizing agents onto fiber surfaces. A certain amount of N element in the PEI sizing agents also resulted in increased percentage of N element to 3.60%. With sizing agents coating onto HSHM-CF surfaces, the detected Si content on the surfaces of HSHM-CF@EP and HSHM-CF@PEI samples also declined to a certain extent.

Table 1 shows O1s/C1s and N1s/C1s atomic ratios obtained from high-resolution XPS. Untreated HSHM-CF sample displayed smaller O1s/C1s (0.05) and N1s/C1s (0) values indicating highly inert surfaces of untreated fibers. When the electrochemical oxidation

Table 1 Surface atomic ratios of untreated HSHM-CF sample, HSHM-CF@O sample, HSHM-CF@EP sample and HSHM-CF@PEI sample

	HSHM-CF	HSHM-CF@O	HSHM-CF@EP	HSHM-CF@PEI
O1s/C1s	0.05	0.21	0.20	0.13
N1s/C1s	0	0.03	0.02	0.04

progressed, polar O and N elements were introduced onto fiber surfaces which resulted in a large extent of rise in the O1s/C1s and N1s/C1s values of HSHM-CF@O sample. As a result, the O1s/C1s value on the surfaces of HSHM-CF@O sample increased by 320% and the N1s/C1s value also increased from 0 to 0.03 compared with untreated HSHM-CF. It could be also observed that the O1s/C1s values of HSHM-CF@EP and HSHM-CF@PEI samples decreased by 5% and 38%, respectively, compared with that of HSHM-CF@O sample. However, the N1s/C1s value of the HSHM-CF@PEI sample increased by 33% compared with that of HSHM-CF@O sample due to the introduction of functional groups of PEI sizing agents.

3.3 Analysis of Surface Functional Groups

High-resolution XPS spectra of the C1s region show that carbon-based functional groups are present on all the samples (Fig. 5). The spectra have each been resolved into five individual component peaks that represent graphitic carbon (284.6 eV), carbon present in alcoholic, phenolic or ether groups (285.6–286.3 eV), carbon in quinone or carbonyl groups bonds (287.0–287.6 eV), carbon in carboxyl or ester groups (288.0–288.8 eV), and carbonate groups (290.4–291.2 eV) [39, 42, 48, 50]. The calculated relative contents of different functional groups on the surfaces of different HSHM-CF samples are shown in Table 2.

Compared with that of untreated HSHM-CF sample, there was a significant increase in the relative content of –C-O group on the surfaces of electrochemically oxidized HSHM-CF@O sample, and the relative content of –COOH group also increased by 122%. As can be seen from Fig. 5 and Table 2, a further increase in the relative content of –C-O group happened to the surfaces of EP-sized HSHM-CF@EP sample and there was also an obvious decrease in the percentage of –COOH group. In comparison with HSHM-CF@O sample, the relative content of -COOH group on the surfaces of HSHM-CF@PEI sample increased by 11%.

To gain a better understanding of changes in functional groups, high-resolution XPS spectra of the O1s region are given in Fig. 6. Deconvolution of the O1s spectra results in four peaks that represent carbonyl oxygen atoms (O_{G1}, 531.0–531.3 eV), carbonyl oxygen atoms in esters, amides, and anhydrides as well as oxygen atoms in hydroxyls or ethers (O_{G2}, 532.1–532.5 eV), ether oxygen atoms in esters and anhydrides (O_{G3}, 533.1–533.5 eV) and oxygen atoms in the carboxyl groups (O_{G4}, 534.1–534.4 eV) [54–56]. Table 3 summarizes the specific area ratios of surface oxygen contributions. According to the data in Fig. 6 and Table 3, untreated HSHM-CF contained three major oxygen species, corresponding to peaks O_{G2}, O_{G1} and O_{G3}. Upon surface electrochemical oxidization, the proportion of the O_{G1} peak corresponding to carbonyl oxygen atoms increased obviously and the relative contribution of the O_{G2} peak decreased sharply.
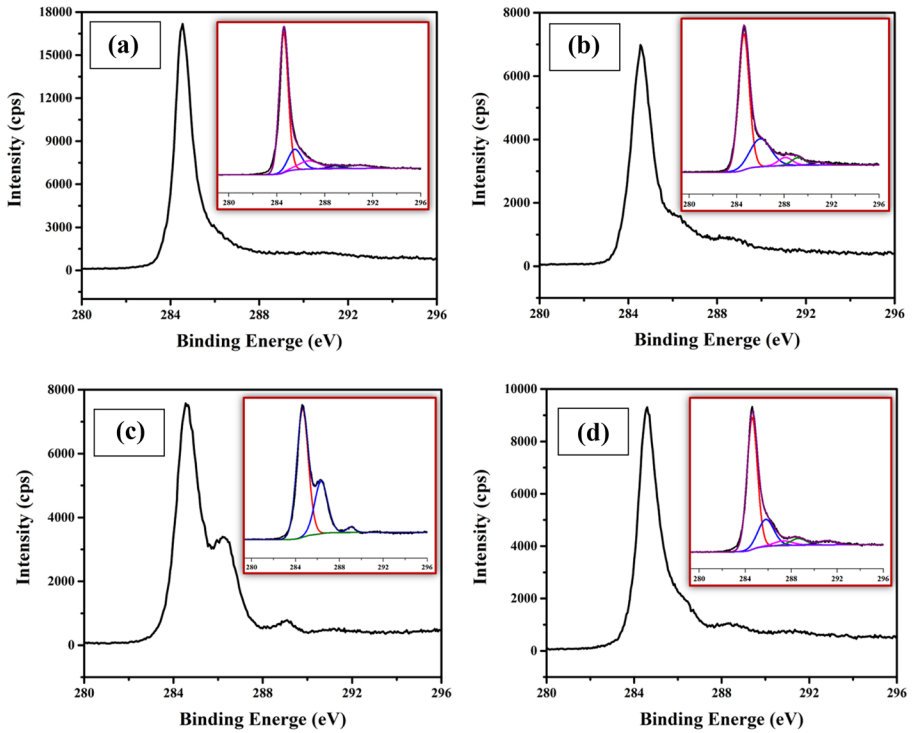
Fig. 5 High resolution XPS C1s spectra and fitted curves of (**a**) untreated HSHM-CF sample, (**b**) HSHM-CF@O sample, (**c**) HSHM-CF@EP sample and (**d**) HSHM-CF@PEI sample

There was little difference in the proportion of O_{G2}, O_{G1} and O_{G3} peaks which indicated that surface electrochemical oxidation led to similar distributions of oxygen atom compositions [55]. In the XPS O1s spectrum of EP-sized HSHM-CF@EP sample, the O_{G2} was the most abundant functionality and the relative contents of O_{G1} and O_{G3} declined to a large extent compared with that of HSHM-CF@O sample. As can be seen from Table 2, the XPS O1s spectrum of HSHM-CF@PEI sample also had similar distributions of oxygen atom compositions.

Table 2 Calculated percentages of graphitic carbon and oxygen-containing functional groups of different samples by XPS C_{1s} spectra

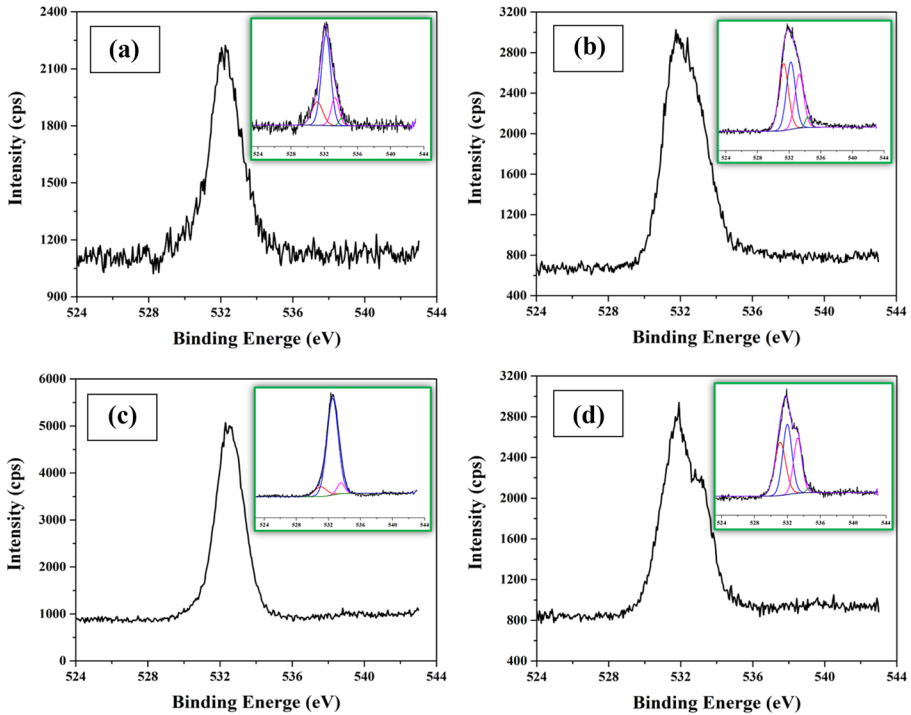| Samples	Relative contents of graphitic and functional groups (%)				
	284.6 eV -C–C	285.6–286.3 eV C-O	287.0–287.6 eV -C=O	288.0–288.8 eV -COOH/ R_1-COO-R_2	290.4–291.2 eV R_1-OCOO-R_2
HSHM-CF	68.59	15.43	9.78	2.04	4.16
HSHM-CF@O	63.32	25.38	5.03	4.53	1.75
HSHM-CF@EP	67.00	30.90	-	2.10	-
HSHM-CF@PEI	66.40	20.69	4.14	5.05	3.73

Fig. 6 High resolution XPS O1s spectra and fitted curves of (**a**) untreated HSHM-CF sample, (**b**) HSHM-CF@O sample, (**c**) HSHM-CF@EP sample and (**d**) HSHM-CF@PEI sample

3.4 Tensile Properties of CFs

Figure 7 shows tensile properties of HSHM-CFs before and after surface treatment, and the error bars correspond to the standard deviations of the strength and modulus data. The tensile strength showed no significant difference between the strength of untreated HSHM-CF sample and electrochemically oxidized HSHM-CF@O sample. Compared with HSHM-CF@O sample, the tensile strength values of HSHM-CF@EP sample and HSHM-CF@PEI sample increased by 2.4% and 4.0%, respectively. More importantly, the strength discrete

Table 3 Calculated percentages of oxygen-containing functional groups of different samples by XPS O_{1s} spectra

Samples	Relative contents of graphitic and functional groups (%)			
	531.0–531.3 eV -C=O	532.1–532.5 eV R-O-C=O, O=C-NH$_2$, O=C–O–C=O, C–OH, R-O-R	533.1–533.5 eV R-O-C=O, O=C–O–C=O	534.1–534.4 eV C-OOH
HSHM-CF	18.83	61.91	16.24	3.02
HSHM-CF@O	35.86	33.97	27.15	3.02
HSHM-CF@EP	9.12	84.48	6.39	—
HSHM-CF@PEI	34.09	37.83	27.05	1.03

Fig. 7 Tensile properties of untreated HSHM-CF sample, HSHM-CF@O sample, HSHM-CF@EP sample and HSHM-CF@PEI sample
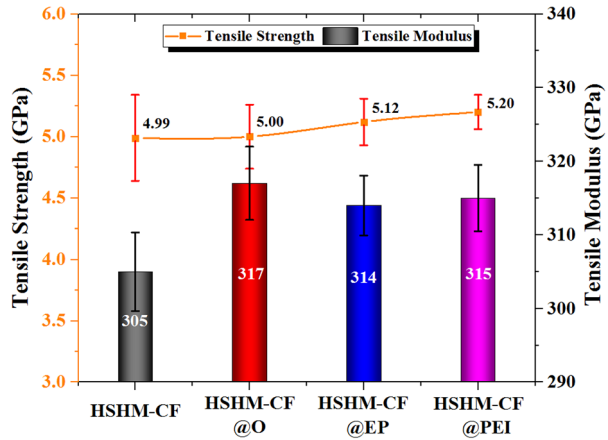
values of HSHM-CF@EP sample and HSHM-CF@PEI sample gradually decreased. Generally speaking, the tensile strength of carbon fiber was strongly affected by internal defects and external surface defects [57], nevertheless, the internal structure of HSHM-CF was unlikely to be oxidized during the electrochemical oxidation. Consequently, changes in the tensile strength of fibers was likely to be a result of the external surface structure [58]. Electrochemical oxidation could get rid of outermost weak boundary and foreign contaminants, which was possibly beneficial to the fiber strength. On the other hand, the chemical etching on fiber surfaces during electrochemical oxidation could bring some damage to the mechanical properties of CFs [42]. The cancellation effect of above two factors resulted in no significant difference between the strength value of untreated HSHM-CF sample and HSHM-CF@O sample. As one kind of brittle fibers, the mechanical properties of CFs also follow the weakest link theory [59], which indicates that the stress is uniform over the entire length of the filament and the largest flaw within the gage section determines its strength in a tensile test [60]. Therefore, increased tensile strength after the EP-sizing and PEI-sizing process possibly resulted in healed surface flaws and inhibited micro-crack initiation [30].

As also can be seen from Fig. 7, the tensile modulus of HSHM-CF@O sample was higher than that of untreated HSHM-CF sample. During the tensile test, fiber tows needed to be pre-impregnated in resin matrix. The wettability between untreated HSHM-CF sample and resin matrix was poor, which was difficult to ensure that each single filament was completely wetted. As a result, the tested tensile modulus of untreated HSHM-CF was possibly lower than the actual value. No significant differences between the modulus values of the HSHM-CF@O, HSHM-CF@EP and HSHM-CF@PEI samples indicated that the electrochemical oxidation and sizing treatment had little effect on the tensile modulus of HSHM-CFs. According to research by Northolt et al. [61], the modulus of CFs depends on three parameters: the in-plane modulus of the graphite plane, the modulus for shear between the graphitic layer planes, and the orientation distribution of these planes. The tensile elastic behavior of CFs is strongly influenced by the manufacturing process, and the shear modulus can be varied over a wide range by heat treatment at elevated temperatures [61]. During the electrochemical oxidation and sizing treatment, the treatment was carried out in the environment of room temperature, which was difficult to affect the internal microcrystalline structure. Therefore, changes in modulus of HSHM-CF before and after surface treatment were not obvious.

3.5 Interfacial Properties of HSHM-CF/PEKK Composites

The effect of electrochemical oxidation and sizing on the interfacial properties of HSHM-CF/PEKK composites was investigated, and Fig. 8 shows the typical flexure load–displacement curves and changes in the ILSS values of HSHM-CF/PEKK composites. As can be seen from Fig. 8, untreated HSHM-CF reinforced PEKK composites revealed typical brittle rupture behavior, and the maximum applied load was merely 610 N (Fig. 8a). The final ILSS value of untreated HSHM-CF reinforced PEKK composites was also as low as 40.7 MPa. After surface electrochemical oxidation, the oxidized HSHM-CF@O sample reinforced PEKK composites demonstrated ductile rupture behavior. The maximum applied load and ILSS value of corresponding composites increased by 84% and 78%, respectively, compared with that of untreated HSHM-CF/PEKK composites. PEKK matrix composites reinforced by EP-sized and PEI-sized samples showed different trends. The maximum applied load decreased from 1122 N for HSHM-CF@O/PEKK composites to 947 N for HSHM-CF@EP/PEKK composites, and the ILSS also decreased from 72.5 MPa to 61.5 MPa, which indicated that EP-coating had an adverse effect on the interfacial properties of HSHM-CF/PEKK composites. On the contrary, both the maximum applied load and ILSS value of HSHM-CF@PEI/PEKK composites increased to the highest values.

In order to better understand the interfacial interaction between HSHM-CFs and PEKK resin in PEKK matrix composites, the SEM images of fractured HSHM-CF/PEKK composites are investigated (as shown in Fig. 9). In untreated HSHM-CF reinforced PEKK composites, there were little residual PEKK resin adhered on surfaces of untreated HSHM-CFs and there were also some pores between fibers and matrix running along the longitudinal direction (Fig. 9a-i). When observed along cross-sectional direction, obvious debonding showed up and the PEKK matrix was broken away from the fibers after the interface failure of the untreated HSHM-CF/PEKK composite(Fig. 9a-ii). Moreover, at high magnification as shown in Fig. 9a-iii, plenty of pores appeared at the fiber-matrix interfaces. It should be noted that the strength of matrix was far smaller than that of reinforcing fibers and the internal micro-pore evolution could result in the failure of composites [62, 63]. As a result, the dominant fracture micro-mechanism for untreated HSHM-CF reinforced PEKK composites was primarily interfacial debonding. In comparison, for the composites reinforced by electrochemically oxidized HSHM-CF@O sample, the fracture microstructure
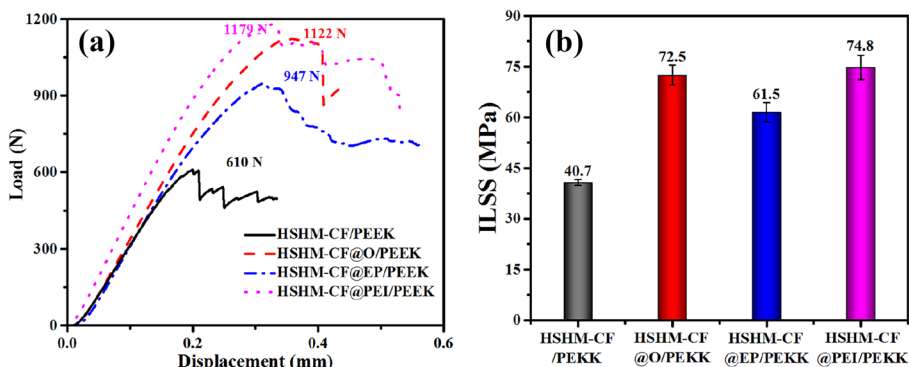

Fig. 8 (**a**) Typical flexure load–displacement curves and (**b**) changes in ILSS values of HSHM-CF/PEKK composites
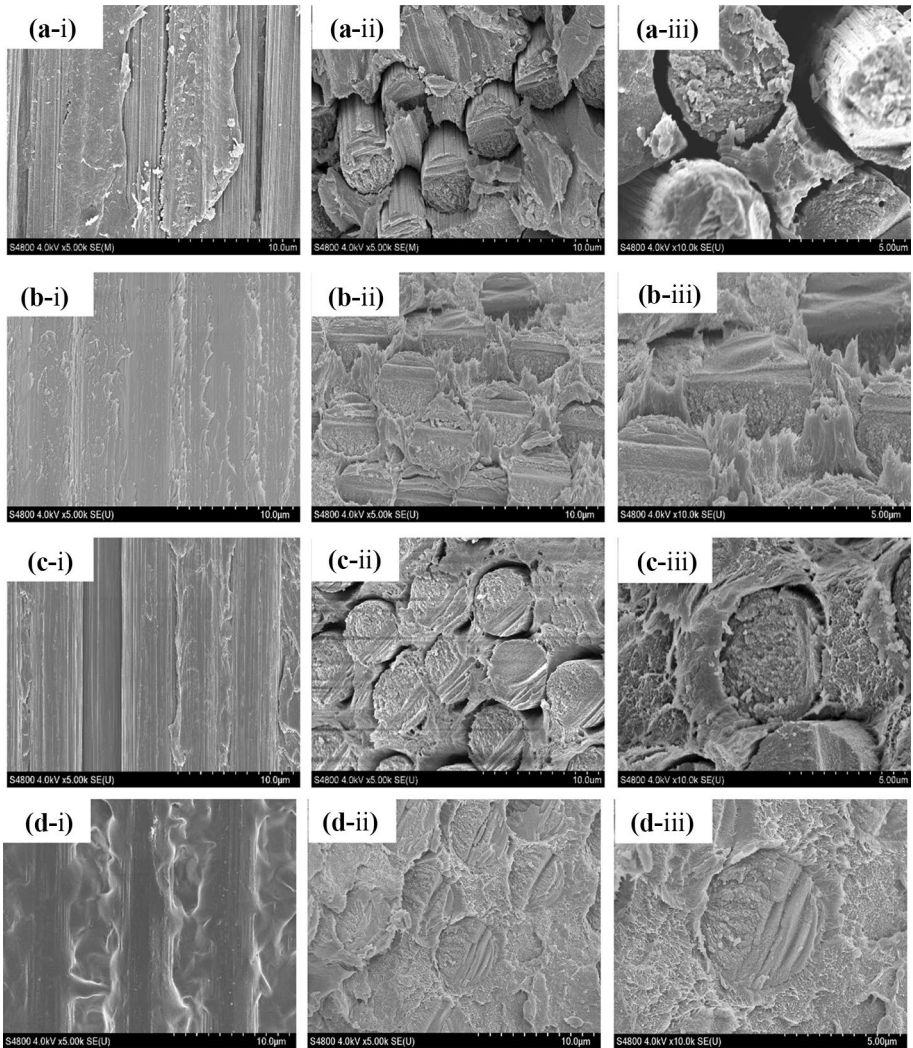
Fig. 9 SEM images of fractured surfaces for PEKK matrix composites reinforced by: (**a** i-iii) untreated HSHM-CF sample, (**b** i-iii) electrochemically oxidized HSHM-CF@O sample, (**c** i-iii) EP-sized HSHM-CF@ EP sample and (**d** i-iii) PEI-sized HSHM-CF@PEI sample

was entirely different. The fibers were adhered by PEKK matrix tightly and the gaps were absent at the fiber-matrix interfaces (Fig. 9b-i). As can be seen from Figs. 9b-ii and b-iii, conspicuous PEKK matrix closely covered around the fiber surfaces along cross-sectional direction. This phenomenon verified that significantly improved adhesion between HSHM-CF@O sample and PEKK matrix occurred after surface electrochemical oxidation.

SEM images of fractured composites reinforced by EP-sized HSHM-CF@EP sample showed that part of PEKK matrix peeled off from the fiber surface and some gaps also appeared between the fibers (Fig. 9c-i). The cross-sectional images of fractured composites clearly indicated that there were obvious cracks and pores at the interfaces although some

matrix still remained on the fiber surfaces (Fig. 9c-ii, c-iii). In comparison, the fibers were adhered by abundant of PEKK matrix without obvious gaps in the composites reinforced by PEI-sized HSHM-CF@PEI samples (Fig. 9d-i). Along the cross-sectional direction of HSHM-CF@PEI/PEKK composites (Fig. 9d-ii,iii), the fibers were tightly covered by the PEKK matrix which confirmed that there was strong interfacial bonding between PEI-sized fibers and PEKK matrix. It could be concluded that introducing PEI sizing agents onto fiber surfaces was beneficial to enhance the interfacial adhesion between HSHM-CFs and PEKK matrix.

3.6 Analysis of Interfacial Enhancement Mechanism

HSHM-CFs without surface oxidation and sizing had lowest O1s/C1s value (Table 1) and highly inert surfaces. The poor wettability of untreated HSHM-CFs by PEKK resin matrix resulted in inadequate interfacial adhesion, thus obvious gaps existed at the interfacial region (Fig. 9a-ii). Defects could induce stress concentration as foreign shear stress was applied to the composites. The failure induced by gaps extended along the interface between the HSHM-CF and PEKK resin, followed by typical debonding failure (Fig. 9a i-iii), which occurred in fiber fracture under small stress [24, 25]. Based on the above experimental results, the possible interfacial reinforcement mechanism of composites reinforced by surface electrochemically oxidized and sized HSHM-CFs was obtained and as shown in Fig. 10.

Compared with untreated HSHM-CFs, the main change of electrochemically oxidized HSHM-CFs lied in that large quantity of oxygen-containing functional groups were introduced onto the fiber surfaces (as shown in Figs. 5 and 6). Introduced reactive groups (e.g. –OH and -COOH) enhanced the opportunity of forming interface interaction between reinforcing fibers and matrix [14]. On the other hand, the elimination of surface weakest boundary and foreign contaminants due to electrochemical oxidation (Fig. 3b), together with the increase of fiber surface activity, could promote impregnation of PEKK matrix into HSHM-CF bundles as well as the improvement of mechanical interlocking. As a result, the enhancement mechanism of PEKK matrix composites reinforced by electrochemically oxidized HSHM-CF@O samples was mainly attributed to chemical reactivity at the interface of the composite and the mechanical interlocking between HSHM-CFs and PEKK matrix. The synergistic mechanism of chemical bonding and mechanical interlocking on the interfacial of CF/EP composites had yet been revealed in our previous published works [41–43].

The ILSS value of PEKK matrix composites reinforced by HSHM-CF@EP sample decreased by 15% compared with that by electrochemically oxidized fibers without sizing (Fig. 8b). It was mainly because of the incompatibility between epoxy sizing agents and PEKK resin matrix. This incompatibility significantly weakened the interfacial reaction at the interface of PEKK matrix composites. However, the ILSS value of HSHM-CF@EP/PEKK composites still increased by 51% compared with that by untreated HSHM-CFs. After the surface treatment, the introduced carboxyl and hydroxyl groups due to electrochemical oxidation could react with the epoxy and hydroxyl groups of EP sizing agents [41, 43, 64], and the carbonyl functionality did not participate in the reactions [65]. However, PEKK chain could diffuse into the sizing layer at high processing temperature and pressure during the preparation the PEKK matrix composites. The carbonyl groups, that did not participating in the chemical reaction between HSHM-CF surface and EP-sizing agents, could possibly form hydrogen bond with PEKK resin matrix. There may also be remaining active carboxyl and hydroxyl groups which could react with the functional
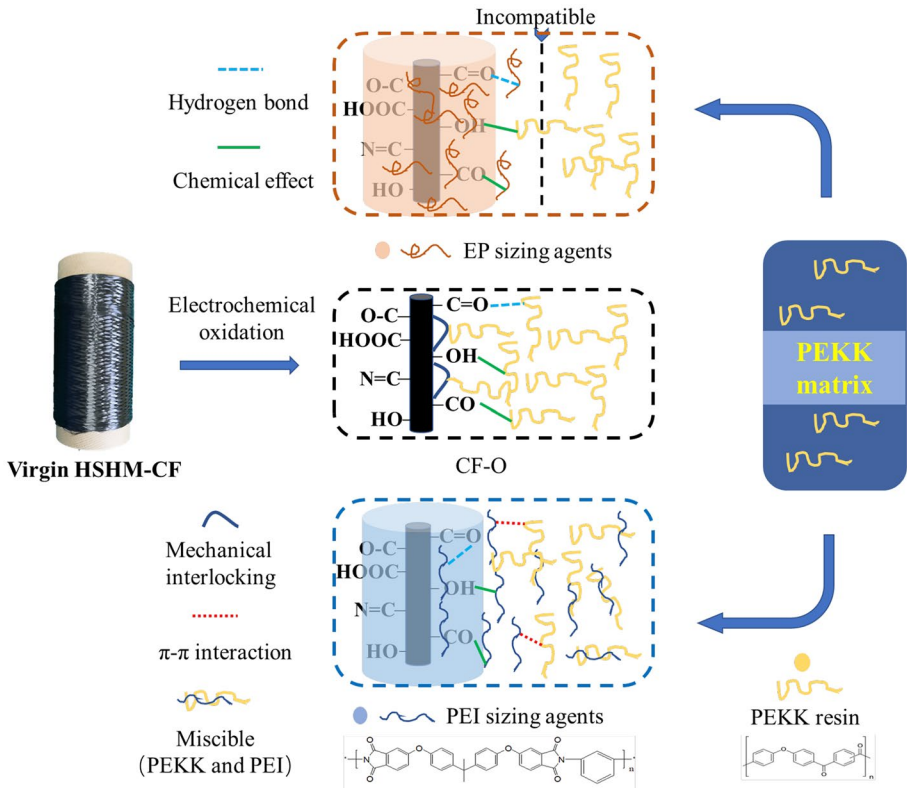
Fig. 10 Schematic of interfacial enhancement mechanism of HSHM-CF/PEKK composites

groups of PEKK matrix. The enhancement mechanism of PEKK matrix composites reinforced by EP-sized HSHM-CFs, therefore, was mainly attributed to hydrogen bond and weak chemical reactions between HSHM-CFs and PEKK matrix.

PEKK matrix composites reinforced by PEI-sized HSHM-CFs had the highest ILSS value, and its enhancement mechanism was more complicated. Increased oxygen-containing functional groups due to electrochemical oxidation could form strong interaction between PEI sizing agents and HSHM-CFs, e.g. hydroxyl groups of oxidized fiber provided electrostatic interactions with five-membered rings in PEI and carboxyl groups of oxidized fiber may form hydrogen bonding with PEI [66]. The relative contents of oxygen-containing functional groups on the surfaces of HSHM-CF@PEI sample were almost consistent with that of HSHM-CF@O sample (as shown in Table 3), which confirmed that the fiber surfaces of HSHM-CF@PEI sample maintained high reactivity with PEKK matrix. On the other hand, PEI sizing agents also had similar chemical structure to PEKK matrix, which could endow good interfacial compatibility with PEKK matrix through diffusion and entanglement between the macromolecular chains. Meantime, the π-π interaction between PEI sizing agents and PEKK, which was similar to that between PEI sizing agents and PEEK [25], could also improve the fiber-matrix interfacial adhesion. In total, the PEI sizing agent serving as a bridge could integrate HSHM-CFs and PEKK matrix closely and result in highest ILSS values of HSHM-CF/PEKK composites.

4 Conclusion

In order to improve interfacial properties of high strength and high modulus carbon fibers (HSHM-CFs) reinforced PEKK composites, a two-step surface treatment including surface electrochemical oxidation followed by sizing process was conducted on HSHM-CFs in the present paper. The electrochemical oxidation could get rid of foreign contaminants on the fiber surface, and further sizing process especially the PEI sizing treatment promoted impregnation of PEKK matrix into HSHM-CF. Much more oxygen-containing groups were introduced onto fiber surfaces after the surface treatment, e.g. the relative content of active oxygen element on fiber surfaces increased by 241% after electrochemical oxidation, which resulted in significant increases in the surface activity. The sizing treatment could result in increased tensile strength, especially for the PEI sized sample, its tensile strength increased by 4.0% compared with surface oxidized sample. However, the sizing treatment had little effect on the tensile modulus of HSHM-CFs. As far as the interfacial properties of HSHM-CF/PEKK composites, the ILSS value of PEKK matrix composites reinforced by electrochemically oxidized HSHM-CFs increased 78% compared with that by untreated HSHM-CFs. Due to the incompatibility of EP sizing agents with PEKK resin matrix, a further EP-sizing treatment after electrochemical oxidation resulted in decreased ILSS value. However, further increases from 72.5 MPa to 74.8 MPa happened to the ILSS value of the composites reinforced by PEI-sized HSHM-CFs, which lied in that the PEI sizing agent serving as a bridge could integrate HSHM-CFs and PEKK matrix closely.

Data Availability The datasets generated during and analysed during the current study are available from the corresponding author on reasonable request.

References

1. Li, C.Y., Strachan, A.: Prediction of PEKK properties related to crystallization by molecular dynamics simulations with a united-atom model. Polymer **174**, 25–32 (2019)
2. Younis, M., Unkovskiy, A., Drexler, T., Qian, J., Wan, G., Spintzyk, S.: The impact of non-thermal plasma on the adhesion of polyetherketoneketone (PEKK) to a veneering composite system. J Mech Behav Biomed Mater **112**, 104065 (2020)
3. Yang, X., Zhao, J., Wu, K., Yang, M., Wu, J., Zhang, X., et al.: Making a strong adhesion between polyetherketoneketone and carbon nanotube fiber through an electro strategy. Compos Sci Technol **177**, 81–87 (2019)
4. Harsha, A.P., Tewari, U.S., Venkatraman, B.: Solid particle erosion behaviour of various polyaryletherketone composites. Wear **254**(7–8), 693–712 (2003)
5. Jin, L., Ball, J., Bremner, T., Sue, H.J.: Crystallization behavior and morphological characterization of poly(ether ether ketone). Polymer **55**(20), 5255–5265 (2014)
6. Coulson, M., Cortés, L.Q., Dantras, E., Lonjon, A., Lacabanne, C.: Dynamic rheological behavior of poly(ether ketone ketone) from solid state to melt state. J Appl Polym Sci **135**(27), 46456 (2018)
7. Cortes, L.Q., Causse, N., Dantras, E., Lonjon, A., Lacabanne, C.: Morphology and dynamical mechanical properties of poly ether ketone (PEKK) with meta phenyl links. J Appl Polym Sci **133**(19), 43396 (2016)
8. Choupin, T., Fayolle, B., Regnier, G., Paris, C., Cinquin, J., Brule, B.: Isothermal crystallization kinetic modeling of poly(etherketoneketone) (PEKK) copolymer. Polymer **111**, 73–82 (2017)

9. Ambalam, M.T., Kumer, D.B., Shanmugamm, D., Jawaid, M.: A review on PEEK composites – Manufacturing methods, properties and applications. Mater Today **33**, 1085–1092 (2020)
10. Hasan, M.M.B., Cherif, C., Foisal, A.B.M., Onggar, T., Hund, R.D., Nocke, A.: Development of conductive coated Polyether ether ketone (PEEK) filament for structural health monitoring of composites. Compos Sci Technol **88**, 76–83 (2013)
11. Chen, M., Ouyang, L., Lu, T., Wang, H., Meng, F., Yang, Y., et al.: Enhanced bioactivity and bacteriostasis of surface fluorinated polyetheretherketone. ACS Appl Mater Interfaces **9**(20), 16824–16833 (2017)
12. Yan, T., Yan, F., Li, S., Li, M., Ao, Y.: Interfacial enhancement of CF/PEEK composites by modifying water-based PEEK-NH2 sizing agent. Compos B Eng **199**, 108258 (2020)
13. Chen, J., Wang, K., Zhao, Y.: Enhanced interfacial interactions of carbon fiber reinforced PEEK composites by regulating PEI and graphene oxide complex sizing at the interface. Compos Sci Technol **154**, 175–186 (2018)
14. Hassan, E.A.M., Ge, D., Yang, L., Zhou, J., Liu, M., Yu, M., et al.: Highly boosting the interlaminar shear strength of CF/PEEK composites via introduction of PEKK onto activated CF. Compos Part A-Appl S **112**, 155–160 (2018)
15. Hassan, E.A.M., Ge, D.T., Zhu, S., Yang, L.L., Zhou, J.F., Yu, M.H.: Enhancing CF/PEEK composites by CF decoration with polyimide and loosely-packed CNT arrays. Compos Part A-Appl S **127**, 105612–105619 (2019)
16. Yuan, B., Chen, Y., Lin, H., Song, Y., Yang, X., Tang, H., et al.: Processing and properties of bioactive surface-porous PEKK. ACS Biomater Sci Eng **2**(6), 977–986 (2016)
17. Tan, S., Su, A., Luo, J., Zhou, E.: Crystallization kinetics of poly(ether ether ketone) (PEEK) from its metastable melt. Polymer **40**(5), 1223–1231 (1999)
18. Choupin, T., Fayolle, B., Régnier, G., Paris, C., Cinquin, J., Brule, B.: Macromolecular modifications of Poly(etherketoneketone) (PEKK) copolymer at the melting state. Polym Degrad Stabil **155**, 103–110 (2018)
19. Yapici, U., Pan, L., Xu, F., Cao, J.M.: Effect of functional groups on interfacial adhesion properties of PEEK/carbon fiber composites. Appl Mechan Mater **598**, 66–72 (2014)
20. Sharma, M., Bijwe, J., MaDer, E., Kunze, K.: Strengthening of CF/PEEK interface to improve the tribological performance in low amplitude oscillating wear mode. Wear **301**(1–2), 735–739 (2013)
21. Jang, J., Kim, H.: Improvement of carbon fiber/PEEK hybrid fabric composites using plasma treatment. Polym Compos **18**(1), 125–132 (1997)
22. Li, J., Sheng, X.H.: Surface oxidation of carbon fibre on tribological properties of PEEK composites. Mater Sci Technol **25**(8), 1051–1056 (2009)
23. Li, J.: Interfacial studies on the ozone and air-oxidation-modified carbon fiber reinforced PEEK composites. Surf Interface Anal **41**(4), 310–315 (2010)
24. Wang, X., Huang, Z., Lai, M., Jiang, L., Zhou, H.: Highly enhancing the interfacial strength of CF/PEEK composites by introducing PAIK onto diazonium functionalized carbon fibers. Appl Surface Sci **510**, 145400 (2020)
25. Hassan, E.A.M., Yang, L., Elagib, T.H.H., Ge, D., Lv, X., Zhou, J., Yu, M., et al.: Synergistic effect of hydrogen bonding and π-π stacking in interface of CF/PEEK composites. Compos B Eng **171**, 70–77 (2019)
26. Wang, S., Yang, Y., Mu, Y., Shi, J., Wang, G.: Synergy of electrochemical grafting and crosslinkable crystalline sizing agent to enhance the interfacial strength of carbon fiber/PEEK composites. Compos Sci Technol **203**, 108562 (2020)
27. Pan, L., Yapici, U.: A comparative study on mechanical properties of carbon fiber/PEEK composites. Adv Compos Mater **25**(4), 359–374 (2016)
28. Wang, T., Jiao, Y., Mi, Z.: Improving the interfacial adhesion of carbon fiber/polyether ether ketone composites by polyimide coating. ChemistrySelect **5**(19), 5507–5514 (2020)
29. Yuan, H., Zhang, S., Lu, C.: Surface modification of carbon fibers by a polyether sulfone emulsion sizing for increased interfacial adhesion with polyether sulfone. Appl Surface Sci **317**, 737–744 (2014)
30. Liu, H., Zhao, Y., Li, N., Zhao, X., Han, X., Li, S., et al.: Enhanced interfacial strength of carbon fiber/PEEK composites using a facile approach via PEI&ZIF-67 synergistic modification. J Mater Res Technol **8**(6), 6289–6300 (2019)
31. Yoo, J.H., Eiss, Y.N.S.: Tribological behavior of blends of polyether ether ketone and polyether imide. Wear **162**, 418–425 (1993)
32. Lee, H.S., Kim, W.N.: Glass transition temperatures and rigid amorphous fraction of poly(ether ether ketone) and poly(ether imide) blends. Polymer **38**(11), 2657–2663 (1997)

33. Giraud, I., Franceschi, S., Perez, E., Lacabanne, C., Dantras, E.: Influence of new thermoplastic sizing agents on the mechanical behavior of poly(ether ketone ketone)/carbon fiber composites. J Appl Polym Sci **132**(38), 42550–42554 (2015)

34. Giraud, I., Franceschi, M.S., Perez, E., Lacabanne, C., Dantras, E.: Preparation of aqueous dispersion of thermoplastic sizing agent for carbon fiber by emulsion/solvent evaporation. Appl Surf Sci **266**, 94–99 (2013)

35. Tan, W., Falzon, B.G.: Modelling the nonlinear behaviour and fracture process of AS4/PEKK thermoplastic composite under shear loading. Compos Sci Technol **126**, 60–77 (2016)

36. Baran, I., Warnet, L.L., Akkerman, R.: Assessment of failure and cohesive zone length in co-consolidated hybrid C/PEKK butt joint. Eng Struct **168**, 420–430 (2018)

37. Whitworth, H.A., Llorente, S.G., Croman, R.B.: Analysis of the fatigue performance of notched and unnotched graphite/thermoplastic composite laminates. J Thermoplast Compos Mater **10**(5), 435–452 (1997)

38. Lin, H.R., Advani, S.G.: Processing models and characterization of thermoplastic composite wound parts. Polym Compos **18**(3), 405–411 (1997)

39. Qian, X., Zhong, J., Zhi, J., Heng, F., Wang, X., Zhang, Y., et al.: Electrochemical surface modification of polyacrylonitrile-based ultrahigh modulus carbon fibers and its effect on the interfacial properties of UHMCF/EP composites. Compos B Eng **164**, 476–484 (2019)

40. Wen, Z., Cheng, X., Zhang, Y., Qian, X.: A two-step carbon fiber surface treatment and its effect on the interfacial properties of CF/EP composites: The electrochemical oxidation followed by grafting of silane coupling agent. Appl Surf Sci **486**, 546–554 (2019)

41. Qian, X., Zhi, J., Chen, L., Jing, H., Zhang, Y.: Effect of low current density electrochemical oxidation on the properties of carbon fiber-reinforced epoxy resin composites. Surf Interface Anal **45**(5), 937–942 (2013)

42. Qian, X., Wang, X., Ouyang, Q., Chen, Y., Yan, Q.: Effect of ammonium-salt solutions on the surface properties of carbon fibers in electrochemical anodic oxidation. Appl Surf Sci **259**, 238–244 (2012)

43. Qian, X., Chen, L., Huang, J., Wang, W., Guan, J.: Effect of carbon fiber surface chemistry on the interfacial properties of carbon fibers/epoxy resin composites. J Reinf Plast Compos **32**(6), 393–401 (2013)

44. Qian, X., Wang, X., OuYang, Q., Chen, Y., Yan, Q.: Surface structural evolvement in electrochemical oxidation and sizing and its effect on carbon fiber/epoxy composites properties. J Reinf Plast Compos **31**(15), 999–1008 (2012)

45. Qian, X., Zhang, Y.G., Wang, X.F., Heng, Y.J., Zhi, J.H.: Effect of carbon fiber surface functionality on the moisture absorption behavior of carbon fiber/epoxy resin composites. Surf Interface Anal **48**(12), 1271–1277 (2016)

46. Mohanty, A.K., Ghosh, A., Sawai, P., Pareek, K., Voit, B.: Electromagnetic interference shielding effectiveness of MWCNT filled poly(ether sulfone) and poly(ether imide) nanocomposites. Polym Eng Sci **54**(11), 2560–2570 (2014)

47. Xia, K., Qin, O., Chen, Y., Wang, X., Wang, L.: Preparation and characterization of lignosulfonate-acrylonitrile copolymer as a novel carbon fiber precursor. ACS Sustain Chem Eng **4**(1), 159–168 (2016)

48. Wen, Z., Qian, X., Zhang, Y., Wang, X., Wang, W., Song, S.: Electrochemical polymerization of carbon fibers and its effect on the interfacial properties of carbon reinforced epoxy resin composites. Compos Part A-Appl S **119**, 21–29 (2019)

49. Qian, X., Zou, R., Ouyang, Q., Wang, X., Zhang, Y.: Surface structural evolvement in the conversion of polyacrylonitrile precursors to carbon fibers. Appl Surf Sci **327**, 246–252 (2015)

50. Yue, Z.R., Jiang, W., Wang, L., Gardner, S.D., Pittman, C.U.: Surface characterization of electrochemically oxidized carbon fibers. Carbon **37**(11), 1785–1796 (1999)

51. Yu, M., Yong, X., Wang, C., Hu, X., Bo, Z., Qiao, K., et al.: Heredity and difference of multiple-scale microstructures in PAN-based carbon fibers and their precursor fibers. J Appl Polym Sci **125**(4), 3159–3166 (2012)

52. Paiva, M.C., Bernardo, C.A., Nardin, M.: Mechanical, surface and interfacial characterisation of pitch and PAN-based carbon fibres. Carbon **38**(9), 1323–1337 (2000)

53. Wang, X.Y., Qian, X., Zhang, Y.G., Wang, X.F., Song, S.L., Zhang, C.: Surface oxidation of PAN-based ultrahigh modulus carbon fibers (UHMCFs) and its effect on the properties of UHMCF/EP composites. Carbon Lett 1–13 (2020)

54. Chiang, Y.C., Lee, C.Y., Lee, H.C.: Surface chemistry of polyacrylonitrile- and rayon-based activated carbon fibers after post-heat treatment. Mater Chem Phys **101**(1), 199–210 (2007)

55. Yoon, C.M., Long, D., Jang, S.M., Qiao, W., Ling, L., Jin, M., et al.: Electrochemical surface oxidation of carbon nanofibers. Carbon **49**(1), 96–105 (2011)

56. Zhang, G., Sun, S., Yang, D., Dodelet, J.P., Sacher, E.: The surface analytical characterization of carbon fibers functionalized by H2SO4/HNO3 treatment. Carbon **46**(2), 196–205 (2008)
57. Newcomb, B.A.: Processing, structure, and properties of carbon fibers. Compos Part A-Appl S **91**, 262–282 (2016)
58. He, D., Soo, V.K., Stojcevski, F., Lipiński, W., Henderson, L.C., Compston, P. et al.: The effect of sizing and surface oxidation on the surface properties and tensile behaviour of recycled carbon fibre: An end-of-life perspective. Compos Part A-Appl S **138**, 106072 (2020)
59. Tetsuya, T., Miyata, T.: Size effect on tensile strength of carbon fibers. Mater Sci Eng **238**(2), 336–342 (1997)
60. Tanaka, F., Okabe, T.: Historical review of processing, microstructures, and mechanical properties of PAN-Based carbon fibers. Compr compos mater 66–85 (2017)
61. Northolt, M.G., Veldhuizen, L.H., Jansen, H.: Tensile deformation of carbon fibers and the relationship with the modulus for shear between the basal planes. Carbon **29**(8), 1267–1279 (1991)
62. Yang, Z., Yan, H.: Multiscale modeling and failure analysis of an 8-harness satin woven composite. Compos Struct **242**, 112186 (2020)
63. Yang, Z., Liu, H.:: Effects of thermal aging on the cyclic thermal shock behavior of oxide/ oxide ceramic matrix composites. Mater Sci Eng **769**, 138494 (2020)
64. Osbeck, S., Bradley, R.H., Liu, C., Idriss, H., Ward, S.: Effect of an ultraviolet/ozone treatment on the surface texture and functional groups on polyacrylonitrile carbon fibres. Carbon **49**(13), 4322–4330 (2011)
65. Weitzsacker, C.L., Xie, M., Drzal, L.T.: Using XPS to investigate fiber matrix chemical interactions in carbon fiber reinforced composites. Surf Interface Anal **25**(2), 53–63 (1997)
66. Victor, N., Sergey, L., Alexey, L., Theo, D., Jose, K., Sergey, L.: Atomistic molecular dynamics simulations of the initial crystallization stage in an SWCNT-polyetherimide nanocomposite. Polymers **9**(11), 548 (2017)

Publisher's Note Springer Nature remains neutral with regard to jurisdictional claims in published maps and institutional affiliations.